Structure
Article

CellPress

Structural and Functional Framework for the Autoinhibition of Nedd4-Family Ubiquitin Ligases

Sara Mari,[1,5] Natalia Ruetalo,[2,5] Elena Maspero,[1] Mira C. Stoffregen,[2] Sebastiano Pasqualato,[3] Simona Polo,[1,4,*] and Silke Wiesner[2,*]
[1]IFOM, Fondazione Istituto FIRC di Oncologia Molecolare, Istituto Europeo di Oncologia, Via Adamello 16, Milan 20139, Italy
[2]Max Planck Institute for Developmental Biology, Spemannstrasse 35, 72076 Tübingen, Germany
[3]Crystallography Unit, Department of Experimental Oncology, European Institute of Oncology, Via Adamello 16, Milan 20139, Italy
[4]Dipartimento di Scienze della Salute, Universita' degli Studi di Milano, Via di Rudini 8, Milan 20122, Italy
[5]Co-first author
*Correspondence: simona.polo@ifom.eu (S.P.), silke.wiesner@tue.mpg.de (S.W.)
http://dx.doi.org/10.1016/j.str.2014.09.006

SUMMARY

Nedd4-family ubiquitin ligases are key regulators of cell surface receptor signaling. Their dysregulation is associated with several human diseases, including cancer. Under normal conditions, the activity of various Nedd4 E3s is controlled through an autoinhibitory interaction of the N-terminal C2 domain with the C-terminal catalytic HECT domain. Here, we report the structural and functional framework for this intramolecular interaction. Our nuclear magnetic resonance (NMR) data and biochemical analyses on Smurf2 and Nedd4 show that the C2 domain has the potential to regulate E3 activity by maintaining the HECT domain in a low-activity state where its ability for transthiolation and noncovalent Ub binding are impaired.

INTRODUCTION

Ubiquitination is one of the most abundant posttranslational modifications in eukaryotes. The ubiquitination reaction is catalyzed by the sequential action of a ubiquitin (Ub)-activating (E1), a conjugating (E2), and a ligating enzyme (E3). Eukaryotic E3s comprise four classes of catalytic domains: HECT, RING, U-box, and RBR (RING between RING). HECT- and RBR-type E3s directly catalyze substrate ubiquitination by a two-step mechanism (Scheffner et al., 1995; Wenzel and Klevit, 2012). First, the catalytic Cys accepts Ub from the E2∼Ub intermediate to form a HECT∼Ub thioester. Then Ub is transferred from the HECT thioester to a Lys residue in the substrate.

The Nedd4 family forms a major group among HECT-type E3s. Nedd4 E3s regulate the trafficking and stability of signaling proteins through mono- and K63-linked poly-ubiquitination (Rotin and Kumar, 2009; Woelk et al., 2006) and thereby ultimately control cellular growth and proliferation. Nedd4 E3s have therefore emerged as crucial regulators of various human diseases (Scheffner and Kumar, 2014). The Nedd4 family is characterized by an N-terminal C2 domain responsible for membrane localization, followed by two to four WW domains that mediate substrate recognition and a bilobal C-terminal HECT domain where the E2 binding N-lobe is connected by a flexible hinge loop to the C-lobe bearing the catalytic Cys (Rotin and Kumar, 2009).

The molecular details of HECT-mediated E3 catalysis have begun to emerge from structural studies of various Nedd4-family members (Kamadurai et al., 2009; Kim et al., 2011; Maspero et al., 2011, 2013; Ogunjimi et al., 2010; Verdecia et al., 2003). Taken together, these studies showed that structural plasticity of the N and C lobe orientation during catalysis is essential for HECT E3 activity. Recently, Kamadurai and colleauges captured the moment when Rsp5, the unique Nedd4 ortholog in yeast, transfers the Ub molecule to a substrate lysine. Following HECT∼Ub thioester formation, the C lobe undergoes a substantial rotation with respect to the N lobe that brings the thioester into spatial proximity to the substrate Lys (Kamadurai et al., 2013).

A second key event in the ubiquitination reaction is the elongation of the Ub chain. The Nedd4-family HECT domains appear to use a sequential Ub addition mechanism where the Ub moiety is added one at a time to the distal end of the growing chain (Kim and Huibregtse, 2009). Consistent with this model, the C-lobe presumably discharges the substrate-conjugated Ub subsequent to ligation and switches back into a conformation that allows it to accept another Ub from the E2-thioester (Maspero et al., 2013). To promote E3 processivity, a noncovalent Ub interaction surface stabilizes the interaction of HECT domains with the growing Ub chain on the substrates (Kim et al., 2011; Maspero et al., 2011; Ogunjimi et al., 2010).

These findings underscore that processes restricting HECT flexibility and locking the N- and C-lobe in particular conformations can regulate ligase activity (Lorenz et al., 2013). Indeed, in the absence of bona fide substrates, a subset of Nedd4-family E3s are kept in a catalytically inactive state by an intramolecular interaction between the N-terminal C2 domain and the C-terminal HECT domain (Wiesner et al., 2007). Although the interaction surface on the C2 domain has been characterized for the Nedd4-family member Smurf2 (Wiesner et al., 2007), the structural and functional details about the C2 domain-binding surface on the catalytic HECT domain are still unknown.

Here, using our recently developed nuclear magnetic resonance (NMR) approach called methionine scanning (Stoffregen et al., 2012), we characterized the C2 domain-binding surface

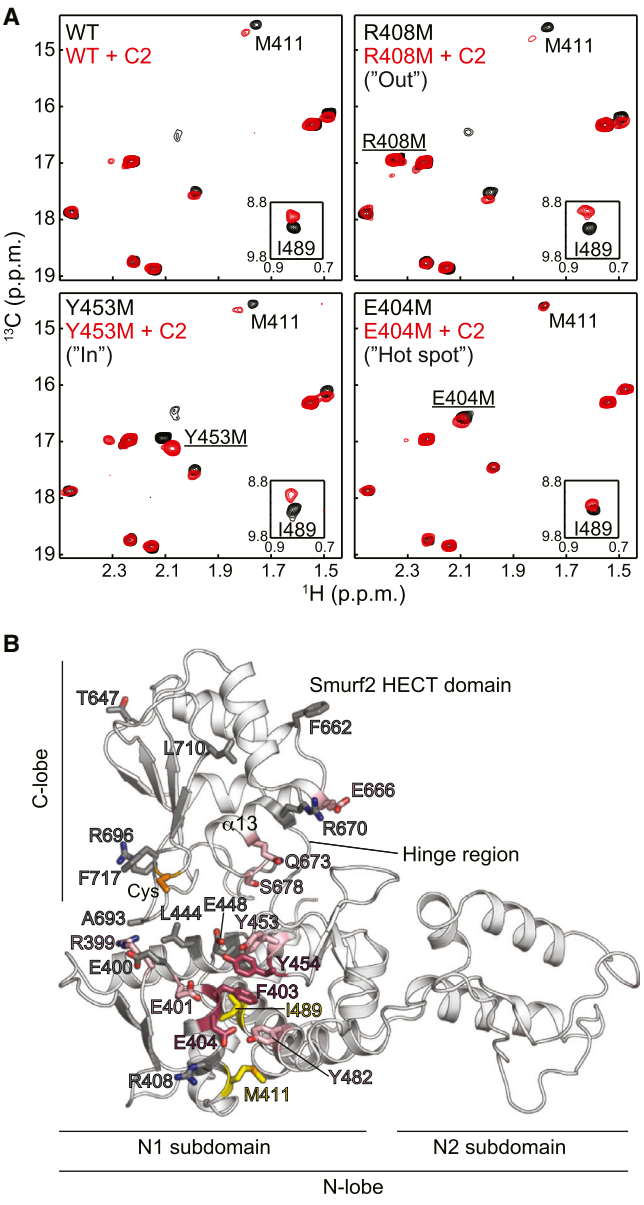

Figure 1. NMR Mapping of the C2 Domain Binding Surface on the Smurf2 HECT Domain

(A) Overlay of selected regions of ^{1}H,^{13}C-methyl TROSY spectra of IM-labeled WT, R408M ("Out"), Y453M ("In"), and E404M ("Hot spot") Smurf2 HECT domain in the absence (black) and presence of a four-fold excess of unlabeled Smurf2 C2 domain (red). Naturally occurring methyl groups experiencing significant CSPs (M411 and I489; IM_{ref}) in the WT protein are labeled in all spectra for reference. Resonances corresponding to the introduced mutation are underlined. The classification of the mutants is based on the CSP analysis presented in Figure S3.

(B) Ribbon representation of the Smurf2 HECT domain (Protein Data Bank [PDB] ID: 1ZVD) color-coded corresponding to the C2 domain binding properties of the Smurf2 HECT domain mutants. "Hot spot" residues are shown in dark pink; "In" and "Out" residues are shown in light pink and dark gray, respectively. Naturally occurring methyl groups with significant CSPs (M411 and I489; IM_{ref}) are shown in yellow; the catalytic Cys is highlighted in orange. See also Figures S1–S3.

of the Smurf2 HECT domain and present molecular insights into this autoinhibitory mechanism shared between a number of Nedd4-family members. Our data on Smurf2 and Nedd4 show that the C2 domain has the potential to downregulate HECT domain activity by interfering with Ub thioester formation and by blocking the noncovalent interaction with Ub, a reaction step critical for ligase processivity.

RESULTS

NMR Mapping of the C2 Binding Surface on the HECT Domain

To explore the molecular basis of HECT domain inhibition, we used NMR spectroscopy to investigate how the C2 domain associates with the catalytic HECT domain in the Smurf2 E3 ligase. Since the poor stability of the Smurf2 HECT domain precluded traditional backbone-directed NMR assignment, we used our recently developed methionine scanning approach (Stoffregen et al., 2012). To this end, we first assigned all naturally occurring Met ε-methyl resonances in the Smurf2 HECT domain by comparing ^{1}H,^{13}C-methyl transverse relaxation optimized (TROSY)-based spectra of the wild-type (WT) protein that was $^{13}CH_3$-labeled exclusively at the Ile δ_1- and Met ε-methyl positions (referred to as IM-labeled protein) with a set of seven IM-labeled Met mutants (Figure S1 available online). In these mutants, all native Met residues were individually mutated to assign the methyl resonance by the disappearance of the corresponding peak in the WT spectrum.

To map the naturally occurring Ile δ_1- and Met ε-methyl groups that participate in C2 domain binding, we next recorded ^{1}H,^{13}C-methyl TROSY spectra of the IM-labeled WT Smurf2 HECT domain in the absence and presence of a 4-fold excess of unlabeled C2 domain. With the assignments of the all-natural Ile δ_1- and Met ε-methyl groups in hand (Figure S1) (Ogunjimi et al., 2010), we can show that the methyl resonances of M411 and I489 (hereafter referred to as IM_{ref}) in the IM-labeled WT Smurf2 HECT domain exhibited significant chemical shift perturbations (CSPs) upon C2 domain binding, while the methyl groups of I402, M449, and I626 showed small, but detectable CSPs (less than a peak width or line broadening; Figure 1A, upper, left; and Figure S2A).

To obtain more detailed information about the amino acids constituting the C2 domain binding pocket and their individual importance for the interaction, we systematically introduced a series of 21 individual Met mutations (referred to as M_{mut}) of solvent-exposed amino acids in proximity to the HECT domain residues that we have identified above as being affected by C2 domain binding (Figure S2B). Using ^{1}H,^{13}C-methyl TROSY experiments, we analyzed the average CSPs of the methyl groups of M_{mut} and IM_{ref} in the WT and mutant Smurf2 HECT domains in the absence and presence of a 4-fold excess of unlabeled C2 domain (Figures 1A and S3). In all Met scanning experiments, the CSPs of the native methyl groups IM_{ref} served as independent internal references for the C2 domain binding properties of the individual mutants to classify the binding properties of the individual Met mutants. Because the measured chemical shifts are highly sensitive to changes in the local chemical environment of the observed atomic nuclei, this method allows us to map a binding surface with per-residue resolution. The individual

Table 1. Summary of C2 Binding Surface Mapping

Smurf2	Nedd4	Location in 3D Structure	C2 Binding[a]	Ub Binding[b]
R399	R549	N-lobe (β1-α1 loop)	*in*	out
E400	A550	N-lobe (β1-α1 loop)	out	out
E401	T551	N-lobe (α1 helix)	*in*	*in*
I402	V552	N-lobe (α1 helix)	*in* (natural Ile)	in
F403	L553	N-lobe (α1 helix)	hot spot	hot spot
E404[c]	E554	N-lobe (α1 helix)	hot spot	*in*
R408	R558	N-lobe (α1 helix)	out	in
M411 (IM_{ref})	M561	N-lobe (α1 helix)	*in* (natural Met)	in
L444	L595	N-lobe (α3 helix)	out	out
E448	E599	N-lobe (α3 helix)	out	out
M449	M600	N-lobe (α3 helix)	*in* (natural Met)	in
Y453[c]	Y604	N-lobe (α3′ helix)	*in*	*in*
Y454	Y605	N-lobe (α3′ helix)	hot spot	hot spot
Y482[d]	Y634	N-lobe (α4 helix)	*in*	hot spot
I489 (IM_{ref})	V641	N-lobe (α4 helix)	*in* (natural Ile)	in
T647	S799	C-lobe (β7-α12 loop)	out	out
F662	M814	C-lobe (α12-α13 loop)	out	out
E666[d]	E818	C-lobe (α13 helix)	*in*	out
R670	R822	C-lobe (α13 helix)	out	out
Q673[d]	Q825	C-lobe (α13 helix)	*in*	out
S678[d]	T830	C-lobe (α13-β8 loop)	*in*	out
A693	N845	C-lobe (α13-β8 loop)	out	out
R696	Q848	C-lobe (α13-β8 loop)	out	out
L710	L861	C-lobe (β8-β9 loop)	out	out
F717	F868	C-lobe (catalytic loop)	out	out

Smurf2 mutants were classified based on their CSPs upon C2 domain addition in NMR experiments as outlined (see Figure S3). The equivalent residues in Nedd4 along with their Ub binding capabilities are indicated (see Figure 4A and Maspero et al., 2011).

[a]Binding capabilities based on the Met scanning study performed in this work.

[b]Binding capabilities based on functional assays (Figure 5A and Maspero et al., 2011), the Nedd4 HECT:Ub crystal structure (PDB ID: 2XBB) (Maspero et al., 2011), and Figure S6B.

[c]Mutations used to examine the functional effects of the C2:HECT interaction in the full-length Smurf2 and Nedd4 enzymes (see Figures 5 and 6).

[d]Mutations that exhibited line-broadening of M_{mut} upon addition of the C2 domain (see Figures S3 and S6A).

Met mutations can have three effects (Stoffregen et al., 2012): one, the mutated residue lies outside the binding pocket resulting in no observable CSP for M_{mut}, but CSPs identical to the WT protein for IM_{ref} (Figure 1A, upper right panel). Two, the mutated residue is involved in binding but not a key residue. Then a CSP is observed for M_{mut}, while the CSPs for IM_{ref} are similar to the WT protein (Figure 1A, lower left panel). Three, the mutated residue is a binding hot spot resulting in no or significantly reduced CSPs for M_{mut} and IM_{ref} because the mutation severely impairs or abolishes the interaction (Figure 1A, lower right panel).

We found that 11 of the 21 Met mutants (E400M, R408M, L444M, E448M, T647M, F662M, R670M, A693M, R696M, L710M, and F717M) showed no significant CSPs (less than half a peak width) for M_{mut}, but CSPs comparable to the WT HECT domain for IM_{ref}. We therefore classified these Met substitutions as being located outside the C2 domain-binding surface ("Out"; Figure S3; Table 1). For seven mutants (R399M, E401M, Y453M, Y482M, E666M, Q673M, and S678M), we found that M_{mut} exhibits a significant change in chemical shift upon addition of the C2 domain, whereas IM_{ref} show CSPs comparable to the WT protein. We thus conclude that these Met substitutions participate in C2 domain binding ("In"; Figure S3; Table 1). Lastly, for three substitutions (F403M, E404M, and Y454M), we observed CSPs for M_{mut} but virtually no CSPs for IM_{ref}. This indicates that these mutations interfere with C2 domain binding and thus can be considered binding hot spots ("Hot spot"; Figure S3; Table 1).

In sum, these data show that the C2 domain-binding surface mainly maps to the larger (N1) subdomain of the N-terminal lobe of the Smurf2 HECT domain (Figure 1B; Figure S4). The binding surface is composed of acidic and aromatic residues with the hot spots clustering in the center of the mapped surface (Figure 1B) corroborating our previous hypothesis that electrostatic and hydrophobic interactions form the basis of the Smurf2 C2:HECT domain interaction (Wiesner et al., 2007).

The C2:HECT Interaction Directly Antagonizes Noncovalent Ub Binding

Structural comparison of the Smurf2 C2 interaction surface with previously determined Ub binding surfaces on HECT domains (French et al., 2009; Kim et al., 2011; Maspero et al., 2011; Ogunjimi et al., 2010) revealed that these interaction sites significantly overlap (Figures 2A and 2B; Figure S4). Directly confirming this observation, we noticed that all naturally occurring Smurf2 Ile and Met residues inside the C2 binding surface (IM_{ref}, Table 1) also exhibited methyl CSPs upon addition of a 4-fold excess of unlabeled Ub to the HECT domain (Figure S5A). Consistent with the different chemical composition of the two ligands, these methyl resonances shift into different directions upon addition of the C2 domain and Ub, respectively. Thus, these residues participate in binding to both the C2 domain and to Ub in a noncovalent manner.

Interestingly, the residues constituting both the C2 and Ub binding pockets are highly conserved across the entire Nedd4 family (Figure S4). To directly prove that the C2 domain interacts with the HECT domain in Nedd4, we recorded $^{1}H,^{15}N$-TROSY NMR spectra of a partially deuterated, ^{15}N-labeled Nedd4 HECT domain in the absence and presence of a 2-fold stoichiometric excess of either unlabeled C2 domain (Figure 2C) or Ub (Figure 2D). As for the Smurf2 HECT domain, numerous resonances in the Nedd4 HECT domain are affected by the presence of the C2 domain and Ub, respectively (Figures 2C and 2D). Given the high sequence similarity between the Smurf2 and Nedd4 enzymes, we also investigated whether the Nedd4 C2 domain interacts with the Smurf2 HECT domain. To this end, we performed $^{1}H,^{13}C$-methyl NMR spectra of an IM-labeled Smurf2 HECT domain in the absence and presence of unlabeled Nedd4 C2 domain. As shown in Figure S5B, the Nedd4 C2 domain interacts with the Smurf2 HECT domain on a surface that includes the same native Ile and Met methyl groups (IM_{ref}) as for the Smurf2 C2 domain. This result further corroborates

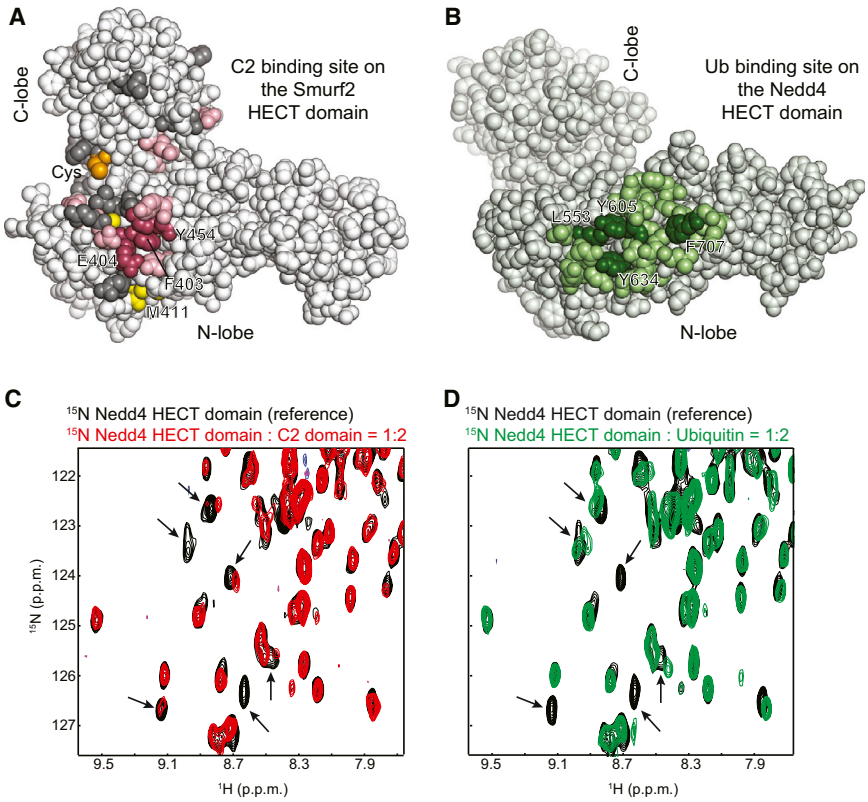

Figure 2. The C2 Interaction Site Overlaps with the Noncovalent Ub Binding Surface

(A) Spheres representation of the Smurf2 HECT domain highlighting the C2 binding surface color-coded as in Figure 1B.

(B) Spheres representation of the Nedd4 HECT domain highlighting residues involved in non-covalent Ub binding (light green) and residues impairing Ub binding (dark green) (PDB ID: 2XBB; Table 1) (Maspero et al., 2011).

(C) Overlay of selected regions of ^{1}H,^{15}N-TROSY spectra of Nedd4 HECT domain in the absence (black) and presence of a 2-fold excess of unlabeled Nedd4 C2 domain (red).

(D) As in (C), but in the absence (black) and presence of a 2-fold excess of unlabeled Ub (green). Resonances marked with arrows are affected by both ligands. See also Figures S4 and S5.

our hypothesis that the Smurf2 and Nedd4 ligases are structurally and functionally highly similar.

To further examine whether the C2 domain may regulate HECT domain activity in Nedd4 in a manner similar to Smurf2 (Wiesner et al., 2007), we next performed in vitro ubiquitination assays using GST-tagged Nedd4 proteins that were expressed recombinantly in *Escherichia coli* as GST-fusions (Figure 3A) or FLAG-tagged Nedd4 proteins expressed in transfected HEK293T cells (Figure 3B). In both cases the Nedd4 ΔC2 and HECT domain enzymes readily incorporated Ub into poly-Ub chains, while the full-length (FL) enzyme showed a considerable delay in the kinetics of autoubiquitination and Ub chain formation (Figures 3A and 3B). Finally, we explored whether the C2 domain functionally interferes with the Ub binding ability of HECT domains. Because various Nedd4-family members including Nedd4 and Smurf2 have been shown to synthesize almost exclusively K63-linked poly-Ub chains (Kim and Huibregtse, 2009; Maspero et al., 2013), we performed pull-down assays with recombinant Nedd4 and Smurf2 enzymes, using the FL proteins, mutants lacking the C2 domain (ΔC2) and the isolated HECT domains, and commercially available K63-linked Ub chains that mimic the physiological reaction product of Nedd4 and Smurf2 catalysis (Maspero et al., 2013) (Figures 3C and 3D). Consistent with our structural analysis, the FL Nedd4 and Smurf2 enzymes are significantly impaired in poly-Ub binding, whereas the isolated HECT domains and the ΔC2 variants efficiently pull down K63-linked poly-Ub chains.

In sum, these results establish that the C2 domain inhibits Nedd4 catalytic activity. In both Nedd4 and Smurf2, C2 domain binding directly blocks the noncovalent Ub binding surface that is important for Ub chain elongation (Kim et al., 2011; Maspero et al., 2011; Ogunjimi et al., 2010).

Mutations in the C2:HECT Interface Release E3 Autoinhibition

To assess the functional importance of the C2:HECT interaction, we generated numerous C2-binding pocket mutants. Guided by the structural data gained for Smurf2 and by sequence conservation (Figure S4), we designed Nedd4 HECT mutations at positions equivalent to those classified as either "In" or "Hot spot" in the Smurf2 HECT domain (Table 1).

To separate the effects of C2 domain binding on E3 activity from deficient Ub chain formation due to impaired Ub binding, we first analyzed the Ub binding capabilities of the isolated Nedd4 WT and mutant HECT domains in Ub pull-down assays. As expected, most of the C2 binding mutants also exhibit reduced Ub binding as compared to the WT HECT domain (Figure 4A), further confirming that the two binding surfaces significantly overlap. Notably, the E554A and Y604A mutants, considered as "Hot spot" and "In" residues in Smurf2 respectively, are able to bind K63-linked poly-Ub chains with similar efficiency as the WT Nedd4 HECT (Figure 4A). Moreover, these two mutants retain WT levels of E2 to E3 transthiolation (Figure 4B) and do not show any deficiencies in auto-ubiquitination assays when used in the context of the isolated HECT (Figure 4C), demonstrating the functional integrity of their catalytic domains.

Having established that the isolated Nedd4 HECT domains carrying the E554A and Y604A mutations in the C2 binding surface are fully functional, we next examined the enzymatic activities of these Nedd4 mutants in the context of the FL enzymes purified at homogeneity. To this end, we performed ubiquitination assays using the bona fide Nedd4 substrate γENaC and full-length WT, ΔC2, and Y604A Nedd4 enzymes. While virtually no ubiquitinated substrate and only a low level of free Ub chains were detected at later time points for the full-length WT Nedd4 protein, both deletion of the C2 domain and the Y604A mutation

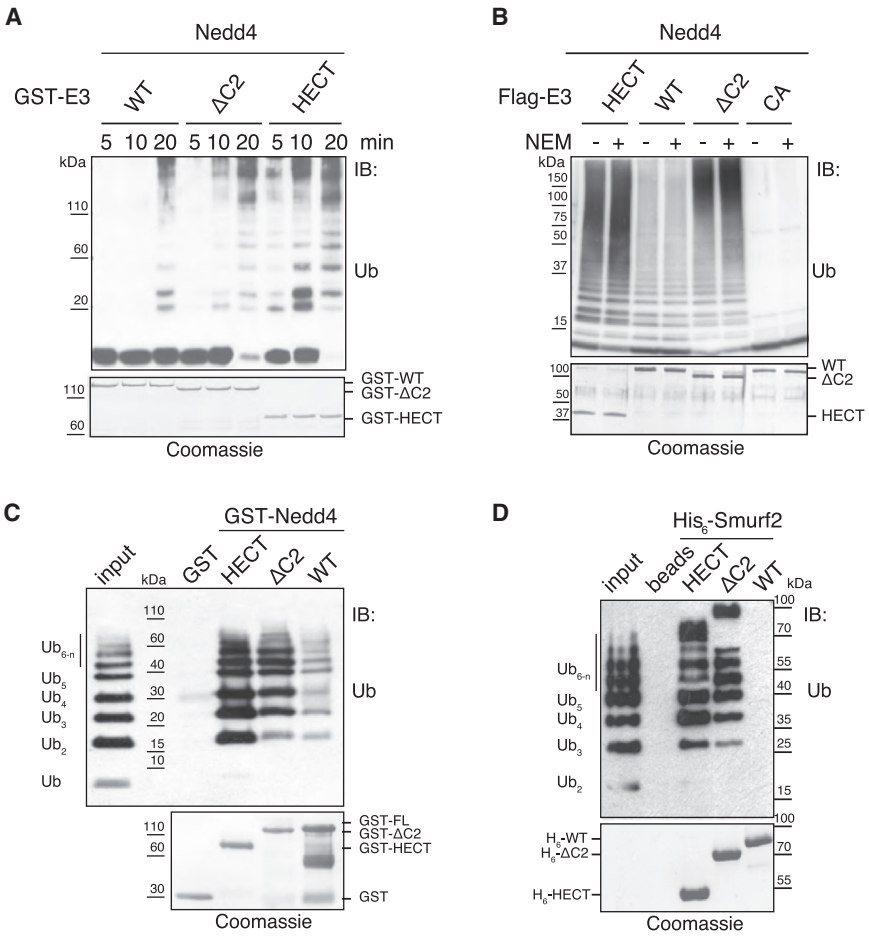

Figure 3. C2 Domain Binding Impairs the Ability of the HECT Domain to Interact Non-covalently with Ub

(A) In vitro ubiquitination assay using the indicated bacterially expressed and purified Nedd4 GST-fusions immobilized on glutathione beads. The beads were separated from the supernatant after the indicated time points. The supernatant was loaded on an 11% Tris-Tricine gel to analyze free Ub chain formation by immunoblot (IB) with α-Ub antibody (top). Equivalent protein levels in the starting material were confirmed by Coomassie staining (bottom).

(B) In vitro ubiquitination assay using the indicated Flag-tagged Nedd4 proteins purified from HEK293T cell lysates and treated with or without NEM. CA, C867A catalytically inactive mutant. Reactions were stopped after 20 min and loaded on a 4%–20% gradient gel. Autoubiquitination and free Ub chain formation were detected by immunoblot (IB) with α-Ub antibody (top). Equivalent protein levels in the starting material were confirmed by Coomassie staining (bottom).

(C) GST pull-down assay with the indicated Nedd4 proteins. GST-fusion proteins were incubated for 2 hr at 4°C in YY buffer with synthetic K63-polyUb chains. Detection as in (A).

(D) Pull-down assay as in (C), but with the indicated His_6-tagged Smurf2 proteins.

strongly enhance the kinetics of substrate ubiquitination and free Ub chain formation (Figure 5A).

We also tested the Ub chain formation capabilities in the absence of a bona fide substrate for the FL E554A and Y604A Nedd4 mutants along with the I36A/L37A double mutations in the C2 domain, because the equivalent positions in Smurf2 have previously been shown to activate the FL enzyme by interfering with the C2:HECT interaction (Wiesner et al., 2007). As shown in Figure 5B, in contrast to the limited efficiency of the WT enzyme, all FL proteins carrying mutations in the C2:HECT interface form Ub chains as efficiently as the enzyme lacking the C2 domain (ΔC2). Lastly, we obtained consistent results for Smurf2, where the "In" Y453A mutant is virtually as active as the ΔC2 enzyme in autoubiquitination assays, whereas only low levels of autoubiquitinated Smurf2 were observed for the full-length WT enzyme (Figure 5C).

We conclude that mutations in the HECT domain interfering with the C2:HECT interaction activate the full-length Nedd4 and Smurf2 enzymes by releasing C2-mediated autoinhibition.

The C2 Domain Impairs HECT∼Ub Thioester Formation

We have previously shown for Smurf2 that deletion of the C2 domain enables Ub thioester formation (Wiesner et al., 2007). To corroborate this finding and to investigate whether this mechanism is shared between Nedd4 and Smurf2, we performed transthiolation assays with WT Nedd4 and the ΔC2 and Y604A mutants. As shown in Figure 6A, WT Nedd4 exhibits a delayed transthiolation kinetics, while the ΔC2 enzyme readily forms E3∼Ub thioester adducts. Of note, the Ub moiety is then transferred on lysine(s) of the enzyme as demonstrated by the appearance of ubiquitinated species that are resistant to dithiothreitol (DTT) treatment (Figure 6A, middle panel). Strikingly, the kinetics of thioester formation for the Y604A mutant is comparable to the ΔC2 enzyme, further confirming that this single point mutant is capable of releasing the C2-mediated inhibition leading to E3 activation. We obtained consistent results for Smurf2 where the ΔC2 and Y453A gain-of-function mutants formed the Ub thioester more efficiently than the WT protein (Figure 6B). These results are in full agreement with our previous observations on Smurf2 (Wiesner et al., 2007) and demonstrate that in both Nedd4 and Smurf2, the C2 domain maintains the HECT domain in a conformation that impairs the Ub transthiolation process from the E2 to the E3.

Interestingly, we observed that three Met mutations (E666M, Q673M, and S678M) that we classified as "In" residues in our Met scanning studies mapped to the C-lobe of the Smurf2 HECT domain (Table 1; Figure S6A). These three residues are located in or close to the α13-helix and are spatially quite distant from the other "In"/"Hot spot" Met mutants of the N-lobe in the X-ray structure of the Smurf2 HECT domain (Ogunjimi et al., 2005) (Figures 1B and S6B). To explore whether the N and C lobes can adopt a conformation where all residues involved in C2 domain binding form a continuous C2 interaction surface, we calculated structural models of the Smurf2 HECT domain

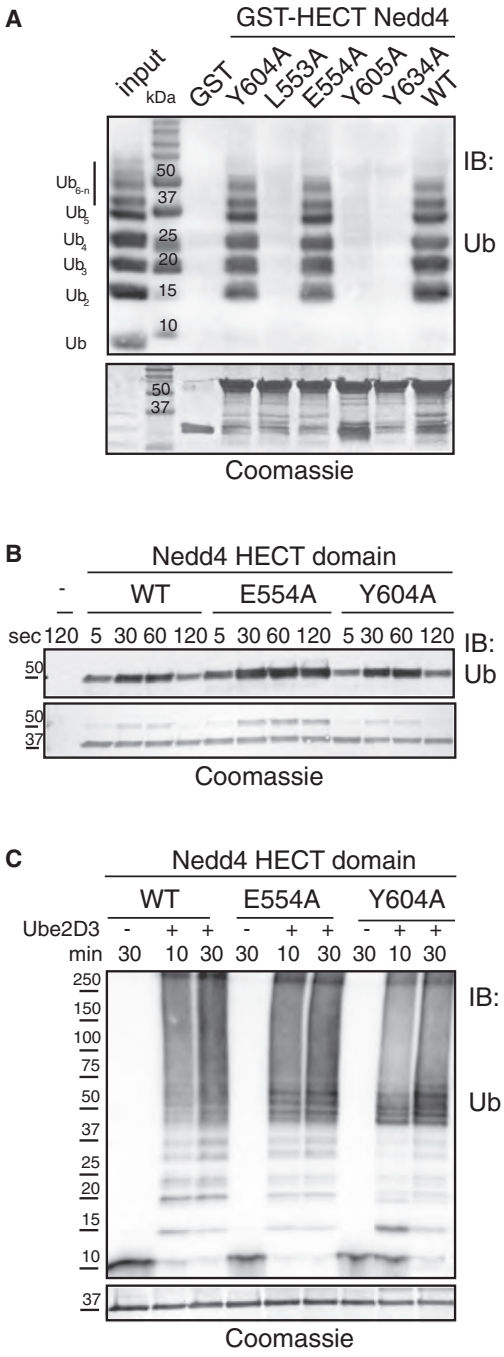

Figure 4. Functional Characterization of Mutations in the C2:HECT Interface in the Context of the Nedd4 HECT Domain

(A) GST pull-down assays with the isolated Nedd4 HECT domains carrying point mutations in the C2 binding surface. E554A and Y604A HECT mutants show K63-polyUb chains binding level similar to Nedd4 HECT WT protein. IB and Coomassie as indicated.

(B) Transthiolation reaction performed with bacterially expressed Nedd4 HECT WT and point mutants. HECT thioester formation was monitored after quenching the reaction at different time points by addition of Laemmli buffer without reducing agent. IB and Coomassie as indicated.

(C) In vitro ubiquitination assays of the Nedd4 HECT WT and point mutants. Reactions were carried out for the indicated time points. IB and Coomassie as indicated.

using the structure determination program CNS (Brünger et al., 1998). Taking the well-established flexibility of the hinge region into account, our modeling efforts focused on a re-orientation of the C lobe with respect to the N lobe using the observed CSPs as experimental restraints for data-driven modeling (Dominguez et al., 2003; Long et al., 2005). Indeed, in the ensemble of ten modeled structures the C lobe residues E666, Q673, and S678 form a continuous C2-interaction surface with the residues mapped on the N1 subdomain (Figures S6C and S6D) and extend the negatively charged surface patch on the HECT domain to accommodate the mainly positively charged residues of the C2 domain (Figure S6E). Importantly, in the modeled conformations, the catalytic Cys in the C lobe would be spatially too remote from the E2 to accept the Ub from the E2 thioester (Figure S6F), offering a structural basis for the defects in Ub transthiolation observed for the WT Smurf2 and Nedd4 enzymes.

Overall, our NMR and biochemical analyses reveal that the C2 domain has the potential to downregulate HECT domain activity on two levels: C2 domain binding interferes with Ub transthiolation and blocks noncovalent Ub binding to the N lobe, a reaction step critical for Ub chain elongation (Figure 7).

DISCUSSION

E3 ligases have emerged as promising targets for drug discovery because they are the first enzymes in the ubiquitination reaction chain that interact with substrates. Thereby E3s are capable of conferring a high degree of specificity and selectivity toward target substrates in cells. E3 activities are tightly regulated on a variety of levels including cooperation with E2 enzyme(s), substrate recognition, E3 processivity, interaction with auxiliary factors as well as Ub and Ub-like proteins, and intramolecular interactions (Duda et al., 2011; Kim et al., 2011; Maspero et al., 2011; Meyer and Rape, 2011; Ogunjimi et al., 2005; Rotin and Kumar, 2009; Wiesner et al., 2007). Despite the broad spectrum of regulatory mechanisms, surprisingly little has been revealed so far at the detailed structural level about how inter- and intramolecular interactions modulate Ub ligase activity. This particularly holds true for interactions that involve the catalytic domains themselves.

Nedd4-family Ub ligases have a common modular architecture containing a C2 domain, two to four WW domains, and a catalytic HECT domain. This domain architecture is conserved across all eukaryotic species, including yeast. Evidence is mounting that the C2 and WW domains of Nedd4-family ligases play dual roles in regulating E3 function: they repress E3 activity in an autoinhibitory manner (Gallagher et al., 2006; Wang et al., 2010; Wiesner et al., 2007), and they target the E3s to their substrates and subcellular locations, thereby promoting ligase activation (Kavsak et al., 2000; Lu et al., 2011; Plant et al., 1997).

Despite the conserved domain architecture, Nedd4-family E3s seem to have evolved distinct modes of autoregulation (Gallagher et al., 2006; Wiesner et al., 2007). The Nedd4-family members Smurf2, Nedd4, Nedd4L, and WWP2 are negatively regulated under basal conditions through an intramolecular interaction involving the C2 and HECT domains to protect themselves and their substrates from premature ubiquitination (Wang et al., 2010; Wiesner et al., 2007). Apparently, this autoinhibitory mechanism does not occur in Smurf1, Itch (AIP4), and Rsp5

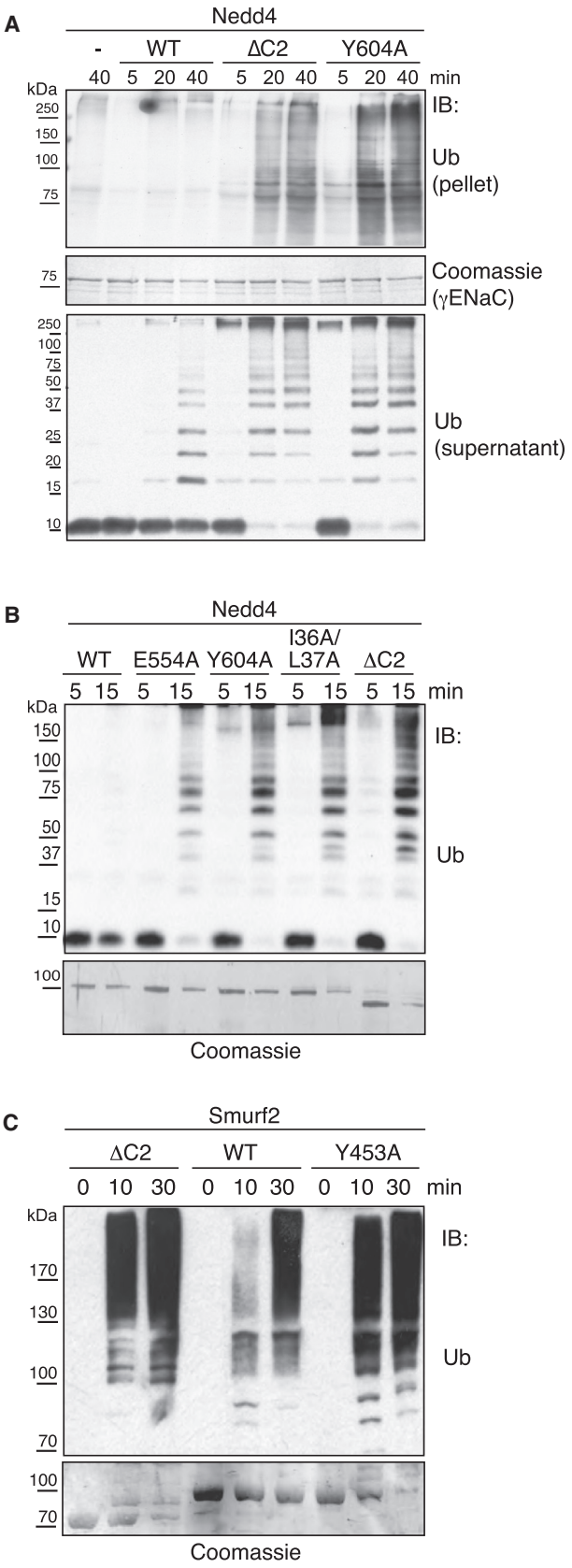

Figure 5. Mutations in the C2:HECT Interface Release E3 Autoinhibition

(A) In vitro ubiquitination assays with GST-tagged γENaC, attached to glutathione beads, as bona fide substrate and the indicated bacterially expressed Nedd4 proteins. The beads containing the substrate were separated from the supernatant after the indicated time points. The washed beads ("pellet") and the supernatant were loaded on loaded on separate SDS-PAGE gels to analyze substrate ubiquitination ("pellet") and free Ub chain formation ("supernatant") by immunoblot (IB) with α-Ub antibody. Equivalent protein levels in the starting material were confirmed by Coomassie staining (middle).

(B) In vitro ubiquitination assay using the indicated bacterially expressed and purified Nedd4 proteins. Reactions were stopped after the indicated time points and loaded on an SDS-PAGE gel to analyze Nedd4 autoubiquitination and free Ub chain formation by IB with α-Ub antibody (top). Coomassie staining (bottom) as in (A).

(C) In vitro autoubiquitination assays with the indicated bacterially expressed Smurf2 full-length WT and mutant proteins. Reactions and detection as indicated.

(Lu et al., 2011; Wiesner et al., 2007). Whereas Itch activity is downregulated by an intramolecular interaction of the region containing the WW domains with the HECT domain (Gallagher et al., 2006), it is yet to be determined if and how Smurf1 and Rsp5 activity is controlled through autoinhibition. Given the high degree of sequence similarity within the interaction and catalytic domains (Figure S4), it will be important to decipher the structural principles governing Nedd4-family E3 inhibition to fully understand the functions of these enzymes and to capitalize on their differential regulation for the design of highly specific pharmaceutical inhibitors, because many Nedd4-family members play important roles in cancer development (Chen and Matesic, 2007; Scheffner and Kumar, 2014).

Here, we have characterized on a structural and functional level the role of the C2 domain in regulating HECT domain activity in the Nedd4-family members Smurf2 and Nedd4. We mapped the C2 binding surface on the Smurf2 HECT domain using our recently developed Met scanning approach (Stoffregen et al., 2012). Methyl NMR spectroscopy has emerged as a powerful tool to study protein structure and interactions. Methyl groups are highly sensitive to changes in their chemical environment so that even slight side-chain rearrangements underneath the binding surface will lead to small but detectable CSPs, as observed for the Smurf2 I402, M449, and I626 residues upon C2 domain binding (Figure S2). In general, methyl groups are evenly distributed in protein structures reducing the risk for NMR invisible regions. Nonetheless, we have introduced in our studies methyl reporters in regions with sparse methyl groups to minimize the possibility of missing, for example, allosteric effects.

Our Met scanning studies have uncovered that the inhibitory C2:HECT interaction occurs mainly on the HECT N lobe and disclosed three highly conserved binding hot spots clustering in the center of the interaction surface (Figure 1). Our structural and biochemical analyses reveal that the C2 domain has the potential to act on HECT domain function in at least two ways: C2 domain binding restricts the C lobe in a conformation that is incompatible with E2 to E3 transthiolation (Figures 6 and S6F) and partially buries the noncovalent Ub binding surface on the N lobe of the HECT domain that is important for E3 processivity (Figures 2, 3C, and 3D). Finally, we demonstrate that mutations in the C2-HECT interface in Smurf2 and Nedd4 lead to robust E3 activation (Figures 5 and 6).

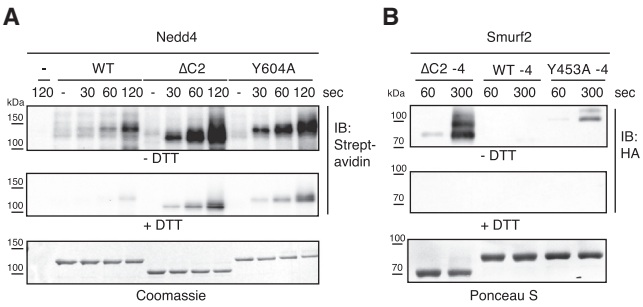

Figure 6. Mutations in the C2:HECT Interface Enhance Ub Thioester Formation

(A) Transthiolation reaction performed with bacterially expressed Nedd4 WT, ΔC2 and Y604A point mutant. HECT thioester formation was monitored after quenching the reaction at different time points by addition of Laemmli buffer without reducing agent. IB and Coomassie as indicated.

(B) Thioester assays were performed with ΔC2, WT, and Y453A Smurf2 truncated by four residues from the C termini ("−4") expressed in bacteria and purified as His_6-fusion proteins. To better visualize the reduction-sensitive Ub thioester, the Smurf2 WT, ΔC2, and HECT domain enzymes were truncated by four residues from their C termini ("−4") as deletion of the conserved −4 Phe position severely impairs HECT-mediated Ub isopeptide-linkage without affecting thioester formation (Salvat et al., 2004). Reactions were stopped at the indicated time points. Ub-modified proteins were detected by immunoblotting with α-HA antibody against HA-tagged Ub, whereas levels of unmodified proteins were visualized by Ponceau S staining.

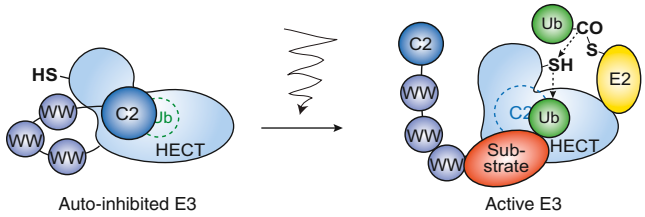

Figure 7. Model for the C2-Mediated Regulation of Smurf2 and Nedd4

Left: the autoinhibited form of the full-length enzymes where the C2 domain induces a catalytic incompetent conformation of the HECT domain. The C2 binding surface overlaps with the noncovalent Ub interaction surface. Specific signaling mechanisms may lead to full E3 activation by releasing the C2 domain, thus allowing for Ub transthiolation, catalysis and Ub chain elongation (right). See also Figure S6.

The mutants that we have chosen for functional characterization (Nedd4 Y604A and Smurf2 Y453A in Figures 5 and 6) unfortunately do not allow us to separate the effects of the C2 domain on thioester formation from Ub chain elongation. Therefore, we cannot establish from our data whether the C2 domain could inhibit E3 processivity had it not blocked thioester formation in the first place. While finding a mutant that clearly separates the two inhibitory effects is beyond the scope of this study, we notice that several "Hot spot" and "In" residues in the C2 binding surface (Table 1) correspond to mutants that we have already characterized as being defective in enzyme processivity (Maspero et al., 2011). We would therefore predict that some of these mutations in the context of the FL enzyme would enable thioester formation while retaining inhibition of Ub binding and substrate polyubiquitination.

It is also worth noting that although we observe an effective inhibition of ligase activity by the C2 domain, in all our functional assays, the WT Smurf2 and Nedd4 enzymes display low levels of transthiolation and ubiquitination activity (Figures 3A, 3B, 5, and 6). This is most likely a reflection of the C2:HECT interaction being dynamic in nature and as such in an "on" and "off" equilibrium resulting in low level, basal activity. Basal activity in the absence of ligand stimulation is a common phenomenon, for example, in receptor tyrosine kinases (Belov and Mohammadi, 2012). In this case, autoinhibition prevents the kinase from giving rise to a cellular signal rather than fully inactivating the enzyme. A transient dissociation of the C2 domain may thus eventually allow for thioester formation. As long as intermolecular C2 interactions and / or the thioester-linked Ub itself would not interfere with the fast intramolecular re-association of the C2 domain, the C2 domain could then play a role in outcompeting noncovalent Ub binding to inhibit poly-Ub chain formation. Of note, our NMR analyses are fully consistent with the catalytic Cys being spatially too remote from the E2 for transthiolation rather than being buried by the C2 domain and hence inaccessible. Although being difficult to test experimentally, this scenario may explain why the C2 domain has the potential to act on two sequential reaction steps in HECT-mediated ubiquitination.

Our finding that the C2 and Ub binding surfaces in Smurf2 and Nedd4 overlap to a large extent might suggest that monomeric Ub or free polyUb chains could outcompete the C2 domain from the HECT domain. Indeed, the K_d for the non-covalent interaction of monomeric Ub with Nedd4-family HECT domains lies in the range of 10 to 90 μM (Kim et al., 2011; Maspero et al., 2011), whereas the Nedd4 C2 domain displays a 220 μM affinity for the HECT domain *in trans* (Figure S5C). While it is difficult to determine dissociation constants *in cis*, we observed in our in vitro ubiquitination assays that even a large stoichiometric excess of monomeric Ub (see Experimental Procedures) is not sufficient to activate full-length WT Smurf2 (Figures 5C and 6B) (Wiesner et al., 2007). This strongly suggests that *in cis* the C2 domain provides robust "on-site" enzyme repression due to the intra-molecular nature of the C2:HECT interaction.

A critical issue that remains to be addressed is how upstream signaling events may trigger the complete release of the C2 domain, leading to full ligase activation (Polo, 2012). One possible activation mechanism for Smurf2 is the intermolecular interaction with the adaptor protein Smad7. By releasing C2-mediated autoinhibition (Wiesner et al., 2007), stimulating E2 binding and recruiting Smurf targets (Ogunjimi et al., 2005), Smad7 functions at multiple levels to control E3 activity and to ensure specificity in Smurf-catalyzed ubiquitination. In the case of Nedd4, calcium-mediated membrane translocation has been suggested to activate Nedd4 by releasing the C2 domain from the HECT domain (Wang et al., 2010). Another, not mutually exclusive, hypothesis is that posttranslational modifications caused by upstream signaling events may result in the dissociation of the autoinhibitory HECT interaction and thereby activate Nedd4. Although a similar mechanism of regulation was recently demonstrated for the activation of the RING ligase Cbl (Dou et al., 2012) and the Nedd4 family member Itch (Gallagher et al., 2006), this hypothesis awaits future studies for other Nedd4 family members.

EXPERIMENTAL PROCEDURES

Protein Purification for Biochemical Assays

Nedd4 GST fusion proteins were expressed in *E. coli* BL21(DE3) and purified by affinity chromatography. Where indicated, GST fusion proteins were cleaved with PreScission protease (GE Healthcare). Ube2D3 (UbcH5c), UbcH7, and all Smurf2 proteins used in biochemical assays were produced as a His_6-fusion protein and purified on Ni-NTA agarose beads (QIAGEN, manufacturer's protocol) followed by size-exclusion chromatography (Wiesner et al., 2007). For Ub pull-down experiments, GST-Nedd4 and His_6-fusion Smurf2 proteins were used, while the His_6-tag was cleaved with TEV protease for UbcH7 or when proteins were used in autoubiquitination assays. Additional details are described in the Supplemental Experimental Procedures.

Purification of Nedd4 Proteins Overexpressed in HEK293T Cells

HEK293T cells were transfected with various Flag Nedd4 constructs using the calcium phosphate procedure. Lysates prepared in RIPA buffer (50 mM Tris-HCl pH 7.6, 150 mM NaCl, 1% NP-40, 0.1% SDS, 0.5% deoxycholic acid, 20 mM Na pyrophosphate pH 7.5, 50 mM NaF, 2 mM phenylmethanesulfonylfluoride, 10 mM Na vanadate, and protease inhibitor cocktail [Calbiochem]) in the presence or absence of 0.5 mM NEM were incubated with α-Flag M2 antibody (2 μg/mg of lysate) and protein G sepharose beads (Zymed) for 2 hr at 4°C on a rocking wheel. Nedd4 immunopreciptated proteins were then washed four times in RIPA buffer, eluted in FLAG elution buffer (300 μg/ml FLAG peptide, 50 mM Tris-HCl pH 7.4, 300 mM NaCl, 5% glycerol), and quantified by Coomassie staining.

Protein Expression and Purification for NMR Spectroscopy

All proteins for NMR spectroscopy were expressed in *E. coli* BL21-CodonPlus (DE3) RIL cells (Stratagene) and purified by Ni-affinity and size-exclusion chromatography (Wiesner et al., 2007). Unlabeled Smurf2 and Nedd4 C2 domains were expressed in Luria broth medium, while IM-labeled Smurf2 HECT domain and partially deuterated, ^{15}N-labeled Nedd4 HECT domains were expressed in 100% D_2O or ~90/10% D_2O/H_2O M9 minimal medium, respectively, as described (Stoffregen et al., 2012). Both the Smurf2 C2 and HECT domain were buffer exchanged into NMR buffer (99% D_2O, 20 mM Na phosphate pH 6.5, 150 mM NaCl, 1 mM DTT, and 0.03% NaN_3) for methyl CSP experiments, whereas 50 mM Tris-HCl pH 7.0, 200 mM NaCl, 2.5% glycerol, and 1 mM DTT was used as NMR buffer for the Nedd4 C2 and HECT domains.

ILVM-labeled Smurf2 HECT domain was prepared analogous to IM-labeled proteins except that, in addition to $^{13}CH_3$-methyl labeled methionine and α-ketobutyric acid, α-ketoisovaleric acid (100 mg/l; where only one of the two isopropyl methyl groups was $^{13}CH_3$-labeled, the other $^{12}CD_3$-labeled) was added after $^1H/^2H$ exchange to the growth medium 1 hour before induction to introduce $^{13}CH_3$-methyl groups in Met, Ile, Leu, and Val as described elsewhere (Tugarinov et al., 2006).

Methionine Scanning and Binding Site Mapping

In total, 21 individual Met point mutants (R399M, E400M, E401M, F403M, E404M, R408M, L444M, E448M, Y453M, Y454M, Y482M, T647M, F662M, E666M, R670M, Q673M, S678M, A693M, R696M, L710M, and F717M) of the Smurf2 HECT domain were generated by site-directed mutagenesis using the QuikChange Site-Directed Mutagenesis protocol (Stratagene). CSP experiments were performed by recording 2D $^1H,^{13}C$-methyl-TROSY spectra of 40 μM IM-labeled WT and mutant Smurf2 HECT domains before and after addition of a four-fold stoichiometric excess of unlabeled Smurf2 C2 domain at 27°C or using a 40 μM ILMV-labeled Smurf2 HECT domain before and after addition of a four-fold stoichiometric excess of unlabeled Ub. Average chemical shift perturbations ($\Delta\delta_{Av} = ((\Delta\delta(^1H))^2 + (\Delta\delta(^{13}C))^2)^{1/2}$) of IM_{ref} (M411 and I489) and M_{mut} observed in the WT Smurf2 HECT domain and the individual methionine substituted proteins upon addition of a 4-fold stoichiometric excess of unlabeled Smurf2 C2 domain were calculated in Hz and used to classify each mutant as described.

For Nedd4, 2D $^1H,^{15}N$-TROSY spectra of 100 μM partially deuterated, ^{15}N-labeled HECT domain samples were recorded at 30°C before and after addition of a 2-fold stoichiometric excess of unlabeled Nedd4 C2 domain and Ub, respectively. All NMR data were collected on an 800 MHz Bruker Avance-III spectrometer, processed and analyzed using the NMRPipe/NMRDraw program suite (Delaglio et al., 1995), and depicted with NMRView (OneMoonScientific).

Ubiquitination Assays

Ubiquitination assays were performed essentially as previously described (Maspero et al., 2013; Wiesner et al., 2007). Nedd4 reaction mixtures were incubated at 37°C and contained purified enzymes (20 nM E1, 250 nM His_6-tagged Ube2D3 [UbcH5c], 250 nM tagged or untagged E3 as indicated), 300 nM substrate (rat γ-ENaC [amino acids 141–646] as GST-fusion protein), and 0.5 or 1 μM Ub (for autoubiquitination or substrate ubiquitination assays) in ubiquitination buffer (25 mM Tris-HCl, pH 7.6, 5 mM $MgCl_2$, 100 mM NaCl, 0.2 μM DTT, 2 mM ATP). GST-tagged Nedd4 proteins or γ-ENaC were used immobilized on glutathione beads. In this case, samples were centrifuged at the indicated time points to separate the beads ("pellet"), containing the ubiquitinated E3s or substrate, from the supernatant, containing unbound enzymes and soluble Ub chains, if produced. The supernatant was directly loaded in 4× Laemmli buffer for SDS-PAGE. The pellet was washed four times in YY buffer (50 mM Na-HEPES pH 7.5, 150 mM NaCl, 1 mM EDTA, 1 mM EGTA, 10% glycerol, 1% Triton X-100) before loading on a SDS-PAGE gel.

For untagged or FLAG-tagged Nedd4 proteins, the reactions were stopped at the different time points by addition of 4× Laemmli buffer and directly loaded on 11% Tris-Tricine or commercial 4%–20% gradient gels (Biorad). For Smurf2, autoubiquitination were performed at room temperature in 25 mM Tris-HCl pH 7.5, 50 mM NaCl, 0.1 mM DTT, 5 mM $MgCl_2$, and 2.5 mM ATP using purified enzymes (0.6 μM E1, 90 μM UbcH7, 2.5 μM Smurf2 proteins) and 65 μM Ub. Smurf2 reaction mixtures were stopped at indicated time points by addition of 4× Laemmli buffer. Samples were loaded for SDS-PAGE on 8% acrylamide gels. Detection was performed by immunoblotting using α-Ub antibody. Membranes were stained with Coomassie after immunoblotting to show equal loading of proteins.

Thioester Assays

Thioester assays were performed essentially as previously described (Maspero et al., 2013; Wiesner et al., 2007). For Nedd4 transthiolation assays, the pulse-chase was performed in two steps. First, 5 μM Ube2D3 were loaded with 10 μM biotinylated Ub in the presence of 100 nM E1 in ubiquitination buffer for 15 min at 37°C and then quenched on ice by a 2-fold dilution with 0.5 M EDTA. Then, the loaded E2 was mixed with the Nedd4 proteins in ubiquitination buffer at a final concentration of 1.4 μM E2, 2.8 μM Ub, and 1 μM E3. Thioester formation at 37°C was monitored by quenching the reaction at different time points in Laemmli buffer without and with 100 mM DTT as reducing agent. Ub-modified proteins were detected by immunoblotting with α-Ub antibody or streptavidin-HRP, whereas levels of unmodified proteins were depicted by Coomassie staining.

For Smurf2, thioester assays were performed at room temperature in ubiquitination buffer using recombinantly expressed and purified enzymes (0.6 μM E1, 9 μM UbcH7, 4 μM His_6-Smurf2 proteins) and 13 μM HA-tagged Ub. To better visualize the reduction-sensitive Ub thioester, the Smurf2 WT, ΔC2 and Y453A enzymes were truncated by four residues from their C termini ("−4") as deletion of the conserved −4 Phe position impairs HECT-mediated Ub isopeptide-linkage without affecting thioester formation (Salvat et al., 2004). The reactions were divided in two after the indicated incubation times and stopped with SDS-PAGE loading buffer without DTT or containing 100 mM DTT. Ub-modified proteins were detected by immunoblotting with α-HA antibody against HA-tagged Ub, whereas levels of unmodified proteins were depicted by Ponceau S staining.

Pull-Down Assays

Bacterially expressed GST-tagged Nedd4 or His_6-tagged Smurf2 proteins were incubated at 2 μM concentration with 250 ng K63-linked poly-Ub chains for 2 hr at 4°C in YY buffer. After four washes with YY buffer, specifically bound proteins were resolved with Tris-Tricine PAGE (11%) and detected by immunoblotting using α-Ub antibody. Membranes were then stained with Coomassie to show equal loading of proteins.

ACCESSION NUMBERS

The BMRB accession number for the Ile δ_1- and Met ε-methyl chemical shift assignments of the Smurf2 HECT domain reported in this work is 25279.

SUPPLEMENTAL INFORMATION

Supplemental Information includes Supplemental Experimental Procedures and six figures and can be found with this article online at http://dx.doi.org/10.1016/j.str.2014.09.006.

AUTHOR CONTRIBUTIONS

S.M., N.R., E.M., S.W., and M.C.S. conducted experiments and data analysis; E.M. and Se.P. participated in experimental design and data analysis; and Si.P. and S.W. conceived of the project, interpreted the results, and wrote the paper.

ACKNOWLEDGMENTS

We thank Eleonora Valentini for performing the fluorescence polarization assay. This work was supported by grants from the Associazione Italiana per la Ricerca sul Cancro (AIRC, IG11627), the European Community (Network of Excellence FP6, 100601-201012), and the European Molecular Biology Organization Young Investigator Program (to S.P.) and by the Max Planck Society and a Marie Curie Reintegration grant (to S.W.; PIRG04-GA-2008-239418 UBLIGATION).

Received: April 6, 2014
Revised: September 3, 2014
Accepted: September 10, 2014
Published: October 30, 2014

REFERENCES

Belov, A.A., and Mohammadi, M. (2012). Grb2, a double-edged sword of receptor tyrosine kinase signaling. Sci. Signal. *5*, pe49.

Brünger, A.T., Adams, P.D., Clore, G.M., DeLano, W.L., Gros, P., Grosse-Kunstleve, R.W., Jiang, J.S., Kuszewski, J., Nilges, M., Pannu, N.S., et al. (1998). Crystallography & NMR system: A new software suite for macromolecular structure determination. Acta Crystallogr. D Biol. Crystallogr. *54*, 905–921.

Chen, C., and Matesic, L.E. (2007). The Nedd4-like family of E3 ubiquitin ligases and cancer. Cancer Metastasis Rev. *26*, 587–604.

Delaglio, F., Grzesiek, S., Vuister, G.W., Zhu, G., Pfeifer, J., and Bax, A. (1995). NMRPipe: a multidimensional spectral processing system based on UNIX pipes. J. Biomol. NMR *6*, 277–293.

Dominguez, C., Boelens, R., and Bonvin, A.M. (2003). HADDOCK: a protein-protein docking approach based on biochemical or biophysical information. J. Am. Chem. Soc. *125*, 1731–1737.

Dou, H., Buetow, L., Hock, A., Sibbet, G.J., Vousden, K.H., and Huang, D.T. (2012). Structural basis for autoinhibition and phosphorylation-dependent activation of c-Cbl. Nat. Struct. Mol. Biol. *19*, 184–192.

Duda, D.M., Scott, D.C., Calabrese, M.F., Zimmerman, E.S., Zheng, N., and Schulman, B.A. (2011). Structural regulation of cullin-RING ubiquitin ligase complexes. Curr. Opin. Struct. Biol. *21*, 257–264.

French, M.E., Kretzmann, B.R., and Hicke, L. (2009). Regulation of the RSP5 ubiquitin ligase by an intrinsic ubiquitin-binding site. J. Biol. Chem. *284*, 12071–12079.

Gallagher, E., Gao, M., Liu, Y.-C., and Karin, M. (2006). Activation of the E3 ubiquitin ligase Itch through a phosphorylation-induced conformational change. Proc. Natl. Acad. Sci. USA *103*, 1717–1722.

Kamadurai, H.B., Souphron, J., Scott, D.C., Duda, D.M., Miller, D.J., Stringer, D., Piper, R.C., and Schulman, B.A. (2009). Insights into ubiquitin transfer cascades from a structure of a UbcH5B approximately ubiquitin-HECT(NEDD4L) complex. Mol. Cell *36*, 1095–1102.

Kamadurai, H.B., Qiu, Y., Deng, A., Harrison, J.S., Macdonald, C., Actis, M., Rodrigues, P., Miller, D.J., Souphron, J., Lewis, S.M., et al. (2013). Mechanism of ubiquitin ligation and lysine prioritization by a HECT E3. eLife *2*, e00828.

Kavsak, P., Rasmussen, R.K., Causing, C.G., Bonni, S., Zhu, H., Thomsen, G.H., Wrana, J.L., Brook, S., York, N., and Smad, S. (2000). Smad7 binds to Smurf2 to form an E3 ubiquitin ligase that targets the TGF beta receptor for degradation. Mol Cell. *6*, 1365–1375.

Kim, H.C., and Huibregtse, J.M. (2009). Polyubiquitination by HECT E3s and the determinants of chain type specificity. Mol. Cell. Biol. *29*, 3307–3318.

Kim, H.C., Steffen, A.M., Oldham, M.L., Chen, J., and Huibregtse, J.M. (2011). Structure and function of a HECT domain ubiquitin-binding site. EMBO Rep. *12*, 334–341.

Long, J.F., Feng, W., Wang, R., Chan, L.N., Ip, F.C., Xia, J., Ip, N.Y., and Zhang, M. (2005). Autoinhibition of X11/Mint scaffold proteins revealed by the closed conformation of the PDZ tandem. Nat. Struct. Mol. Biol. *12*, 722–728.

Lorenz, S., Cantor, A.J., Rape, M., and Kuriyan, J. (2013). Macromolecular juggling by ubiquitylation enzymes. BMC Biol. *11*, 65.

Lu, K., Li, P., Zhang, M., Xing, G., Li, X., Zhou, W., Bartlam, M., Zhang, L., Rao, Z., and He, F. (2011). Pivotal role of the C2 domain of the Smurf1 ubiquitin ligase in substrate selection. J. Biol. Chem. *286*, 16861–16870.

Maspero, E., Mari, S., Valentini, E., Musacchio, A., Fish, A., Pasqualato, S., and Polo, S. (2011). Structure of the HECT:ubiquitin complex and its role in ubiquitin chain elongation. EMBO Rep. *12*, 342–349.

Maspero, E., Valentini, E., Mari, S., Cecatiello, V., Soffientini, P., Pasqualato, S., and Polo, S. (2013). Structure of a ubiquitin-loaded HECT ligase reveals the molecular basis for catalytic priming. Nat. Struct. Mol. Biol. *20*, 696–701.

Meyer, H.J., and Rape, M. (2011). Processive ubiquitin chain formation by the anaphase-promoting complex. Semin. Cell Dev. Biol. *22*, 544–550.

Ogunjimi, A.A., Briant, D.J., Pece-Barbara, N., Le Roy, C., Di Guglielmo, G.M., Kavsak, P., Rasmussen, R.K., Seet, B.T., Sicheri, F., and Wrana, J.L. (2005). Regulation of Smurf2 ubiquitin ligase activity by anchoring the E2 to the HECT domain. Mol. Cell *19*, 297–308.

Ogunjimi, A.A., Wiesner, S., Briant, D.J., Varelas, X., Sicheri, F., Forman-Kay, J., and Wrana, J.L. (2010). The ubiquitin binding region of the Smurf HECT domain facilitates polyubiquitylation and binding of ubiquitylated substrates. J. Biol. Chem. *285*, 6308–6315.

Plant, P.J., Yeger, H., Staub, O., Howard, P., and Rotin, D. (1997). The C2 domain of the ubiquitin protein ligase Nedd4 mediates Ca2+-dependent plasma membrane localization. J. Biol. Chem. *272*, 32329–32336.

Polo, S. (2012). Signaling-mediated control of ubiquitin ligases in endocytosis. BMC Biol. *10*, 25.

Rotin, D., and Kumar, S. (2009). Physiological functions of the HECT family of ubiquitin ligases. Nat. Rev. Mol. Cell Biol. *10*, 398–409.

Salvat, C., Wang, G., Dastur, A., Lyon, N., and Huibregtse, J.M. (2004). The -4 phenylalanine is required for substrate ubiquitination catalyzed by HECT ubiquitin ligases. J. Biol. Chem. *279*, 18935–18943.

Scheffner, M., and Kumar, S. (2014). Mammalian HECT ubiquitin-protein ligases: biological and pathophysiological aspects. Biochim. Biophys. Acta *1843*, 61–74.

Scheffner, M., Nuber, U., and Huibregtse, J.M. (1995). Protein ubiquitination involving an E1-E2-E3 enzyme ubiquitin thioester cascade. Nature *373*, 81–83.

Stoffregen, M.C., Schwer, M.M., Renschler, F.A., and Wiesner, S. (2012). Methionine scanning as an NMR tool for detecting and analyzing biomolecular interaction surfaces. Structure *20*, 573–581.

Tugarinov, V., Kanelis, V., and Kay, L.E. (2006). Isotope labeling strategies for the study of high-molecular-weight proteins by solution NMR spectroscopy. Nat. Protoc. *1*, 749–754.

Verdecia, M.A., Joazeiro, C.A., Wells, N.J., Ferrer, J.-L., Bowman, M.E., Hunter, T., and Noel, J.P. (2003). Conformational flexibility underlies ubiquitin

ligation mediated by the WWP1 HECT domain E3 ligase. Mol. Cell *11*, 249–259.

Wang, J., Peng, Q., Lin, Q., Childress, C., Carey, D., and Yang, W. (2010). Calcium activates Nedd4 E3 ubiquitin ligases by releasing the C2 domain-mediated auto-inhibition. J. Biol. Chem. *285*, 12279–12288.

Wenzel, D.M., and Klevit, R.E. (2012). Following Ariadne's thread: a new perspective on RBR ubiquitin ligases. BMC Biol. *10*, 24.

Wiesner, S., Ogunjimi, A.A., Wang, H.-R., Rotin, D., Sicheri, F., Wrana, J.L., and Forman-Kay, J.D. (2007). Autoinhibition of the HECT-type ubiquitin ligase Smurf2 through its C2 domain. Cell *130*, 651–662.

Woelk, T., Oldrini, B., Maspero, E., Confalonieri, S., Cavallaro, E., Di Fiore, P.P., and Polo, S. (2006). Molecular mechanisms of coupled monoubiquitination. Nat. Cell Biol. *8*, 1246–1254.